ORIGINAL ARTICLE

Simple Versus Complex Approaches to Treating Coronary Bifurcation Lesions: Direct Assessment of Stent Strut Apposition by Optical Coherence Tomography

Pawel Tyczynski,[a,b] Giuseppe Ferrante,[a] Cristina Moreno-Ambroj,[a] Neville Kukreja,[a] Peter Barlis,[a] Elio Pieri[a], Ranil de Silva,[a,c] Kevin Beatt,[d] and Carlo Di Mario[a,c]

[a]Cardiology Department, Royal Brompton Hospital, London, United Kingdom
[b]Department of Interventional Cardiology, Institute of Cardiology, Warsaw, Poland
[c]Imperial College, London, United Kingdom
[d]Cardiology Department, Mayday University Hospital, Croydon, United Kingdom

Introduction and objectives. Stenting of coronary bifurcation lesions carries an increased risk of stent deformation and malapposition. Anatomical and pathological observations indicate that the high stent thrombosis rate in bifurcations is due to malapposition of stent struts.

Methods. Strut apposition was assessed with optical coherence tomography (OCT) in bifurcation lesions treated either using the simple technique of stent implantation in the main vessel only or a complex technique (i.e. Culotte's). A strut was regarded as malapposed if the gap between its endoluminal surface and the vessel wall was greater than its thickness plus an OCT resolution error margin of 15 μm.

Results. Simple and complex (i.e. Culotte's) approaches were used in 17 and 14 patients, respectively. Strut malapposition was significantly more frequent for the half of the bifurcation on the same side as the vessel side branch (median, 46.1%; interquartile range [IQR], 35.3–62.5%) than for the half opposite the side branch (9.1%; IQR, 2.2–21.6%), the distal segment (7.5%; IQR, 2.3–20.2%) or the proximal segment (12.6%; IQR, 7.8–23.1%; *P*<.0001); the gap between strut and vessel wall in malapposed struts was significantly greater in the first segment than the others: 98 μm (IQR, 37–297 μm) vs. 31 μm (IQR, 13–74 μm), 49 μm (IQR, 20–100 μm) and 38 μm (IQR, 17–90 μm), respectively (*P*<.0001). Using the complex technique had no effect on the prevalence of strut malapposition in the four segments relative to the simple technique (*P*=.31) but was associated with a smaller gap in the proximal segment (47 μm vs. 60 μm; *P*=.0008).

Conclusions. In coronary bifurcation lesions, strut malapposition occurred most frequently and was most significant close to the side branch ostium. The use of Culotte's technique did not significantly increase the prevalence of strut malapposition compared with a simple technique.

Correspondence: Prof C. Di Mario,
Cardiology Department. Royal Brompton Hospital,
Sydney Street. London SW3 6NP United Kingdom
E-mail: C.DiMario@rbht.nhs.uk

Received October 20, 2009.
Accepted for publication March 25, 2010.

Key words: *Bifurcation lesion. Percutaneous coronary intervention. Optical coherence tomography.*

Estrategia simple o compleja para lesiones de bifurcaciones coronarias: evaluación inmediata de la aposición de los *struts* del *stent* mediante tomografía de coherencia óptica

Introducción y objetivos. La implantación de *stents* en lesiones de bifurcaciones coronarias comporta un riesgo elevado de deformación y mala aposición del *stent.* Las observaciones anatomopatológicas han atribuido a la mala aposición de los *struts* un papel causal en la elevada tasa de trombosis de los *stents* que se observa en las bifurcaciones.

Métodos. Se evaluó la aposición de los *struts* en las lesiones de bifurcaciones tratadas con una técnica simple de implantación de *stent* solo en el vaso principal o con una técnica compleja (de *culotte*) mediante el empleo de tomografía de coherencia óptica (OCT). La mala aposición de un *strut* se definió por el hecho de que la distancia entre su superficie intraluminal y la pared vascular fuera superior a su grosor más un margen de error de resolución de la OCT de 15 μm.

Resultados. En 17 pacientes se utilizó la estrategia simple y en 14, la técnica compleja (de *culotte*). Los *struts* con mala aposición fueron significativamente más frecuentes y la distancia entre el *strut* y la pared vascular en los casos de mala aposición fue mayor en la mitad de la bifurcación situada hacia la rama lateral (RL) (46,1% [35,3-62,5]) en comparación con la mitad del lado opuesto (9,1% [2,2-21,6]), el segmento distal (7,5% [2,3-20,2]) y el segmento proximal (12,6% [7,8-23,1]; p < 0,0001) (distancias, 98 μm [37-297] frente a 31 μm [13-74], 49 μm [20-100] y 38 μm [17-90], respectivamente; p < 0,0001). El empleo de la técnica compleja no afectó a la prevalencia de *struts* con mala aposición en los 4 segmentos en comparación con la estrategia simple (p = 0,31) y se asoció a una menor distancia *strut*-pared en el segmento proximal (47 frente a 60 μm; p = 0,0008).

Conclusiones. En las lesiones de bifurcaciones coronarias, la mala aposición de los *struts* se produce con mayor frecuencia y es más importante en la zona de origen de la RL. El empleo de la técnica de *culotte* no au-

ABBREVIATIONS

IVUS: intravascular ultrasound
KB: kissing balloon
MV: main vessel
OCT: optical coherence tomography
PCI: percutaneous coronary intervention
SB: side branch

menta de manera significativa la prevalencia de la mala aposición de los *struts* en comparación con una estrategia simple.

Palabras clave: *Lesión de bifurcación. Intervención coronaria percutánea. Tomografía de coherencia óptica.*

INTRODUCTION

While stenting of coronary bifurcation lesions provides good immediate angiographic results, restenosis (even with drug-eluting stents-DES) and stent thrombosis occur more frequently than in simpler lesions. Bifurcation lesions are still considered off-label procedures because of the potential risk of side branch (SB) jailing and stent deformation and malapposition. Pathology observations have indicated potential correlations between stent strut malapposition and stent thrombosis,[1] which may explain why percutaneous coronary intervention (PCI) for bifurcation lesions is an independent risk factor for stent thrombosis.[2] The incidence and predictors of stent thrombosis using different PCI strategies for bifurcation lesions are controversial. Most studies suggest that stent thrombosis is higher in bifurcations treated with two-stents. In the experience of the Milan and Rotterdam groups, Hoye et al. reported a 4.3% rate of stent thrombosis after the "crush" technique.[3] One of the two main randomized trials comparing a simple strategy of stenting the main vessel (MV) only to a complex strategy of stenting both MV and SB, the British Bifurcation Coronary Study: Old, New, and Evolving Strategies (BBC ONE) trial, showed higher stent thrombosis in the two-vessels strategy group.[4] In the Nordic study, however, the 14-month incidence of stent thrombosis was 0.5% in the two-vessel strategy group arm and 2% in the provisional stenting arm.[5]

Two-vessels techniques are expected to induce greater stent deformity and malapposition,[6] but there is no in-vivo confirmation since intravascular ultrasound (IVUS) lacks the ability to precisely detect strut malapposition. Optical coherence tomography (OCT) has higher resolution than IVUS (approximately 10 times), with fewer strut-induced artifacts, and offers precise evaluation of strut apposition in a real-life clinical setting.[7] OCT has proved to be a useful technique in assessing stent apposition after bifurcation treatment using the new dedicated bifurcation stent.[8] Additionally, the results from that study make up a part of the findings in the current complex treatment arm.

The aim of our study was to quantify and compare the apposition of stent struts in bifurcation lesions treated either with a simple technique (MV stenting only) or with a complex technique (stenting of both the MV and the SB using the Culotte technique).[9]

METHODS

Study Population

All consecutive patients who underwent post-procedural OCT examination after stent implantation in bifurcation lesions from January 2006 to September 2008 were enrolled in the study.

Procedure

Provisional MV stenting and dedicated complex techniques have been described previously.[5,10] Six French guiding catheters were used in all cases. High pressure or cutting balloon pre-dilatation as well as post-dilatation with a high-pressure balloon were performed in all cases. After re-wiring into the SB, final kissing balloon (KB) post-dilatation was performed in all complex strategy cases, with the balloons diameters matching and SB diameter and MV diameter distal to the bifurcation. The inflation pressure was at the operator's discretion, based on the type of lesion, the compliance of the balloons, etc. The Culotte technique was used for all complex cases. The choice to use a simple or complex technique was at the operator's discretion, based on the anatomical scenario of the bifurcation lesion. Procedural success was defined as final diameter stenosis <30% in the MV and <50% in the SB by visual assessment with TIMI 3 flow in both the MV and SB.

Pharmacological Treatment and Procedural Devices

Before the procedure, all patients were pretreated with aspirin and 300-600 mg of Clopidogrel. During the procedure, either unfractionated heparin (UFH) or bivalirudin were used: UFH was given to maintain an activated clotting time ≥250 seconds

with an initial bolus of 70 IU/kg, whilst bivalirudin was given according to the patient's body weight. Intravenous or intracoronary administration of glycoprotein IIb/IIIa inhibitors was at the operator's discretion.

Quantitative Angiographic Analysis

All bifurcation lesions were classified according to the Medina classification, depending on the presence or absence of >50% stenosis in the proximal and distal MV and the SB ostium.[11] Quantitative Vascular Arteriography was performed using dedicated 3 segment software (QAngio XA 7.1, Medis Medical Imaging System, Leiden, The Netherlands), as previously described.[12]

OCT Imaging Technique

In this study, an end-hole microcatheter (0.021" Transit™, Cordis Neurovascular, Miami Lakes, FL, USA) was advanced distal to the lesion in the MV over a conventional guide wire, which was then exchanged for the OCT imaging wire. OCT image acquisition (M3 system, LightLab Imaging Inc. Westford, MA, USA) was performed using a non-occlusive technique[13] with continuous flushing of iodixanol (Visipaque™, GE Healthcare, UK) using a power injector (2-5 mL/s) and a pull-back speed set at 3 mm/s. Image acquisition over a 30-35 mm vessel segment was performed in each patient without complication.

OCT Image Analyses

Cross-sectional images from the OCT pull-back were analyzed every 450 μm (every 3 frames). Since the metallic surface of the strut is opaque to infrared light, the abluminal strut surface cannot be seen; therefore, strut malapposition was diagnosed if the distance between the endoluminal surface of even a single strut of the stent and the vessel wall was greater than the thickness of the strut (metal+polymer) plus an additional 15-micron margin of error, consistent with the resolution of OCT.[14] The thickness of the stents used in the study was as follows: Cypher Select-154 μm, Taxus Liberté-127 μm, Endeavor Resolute-95 μm, Xience V-88 μm, Antares-88 μm, Costar-89 μm, and Driver-91 μm.[14] Strut apposition was assessed in four segments: proximal MV segment (extending 8 mm proximal to the first cross-section when the SB was visible), bifurcation (divided into two 180-degree halves towards or opposite the origin of the SB) and distal MV segment (extending 4 mm from the last cross-section when the SB was visible) (Figures 1 and 2). In order to unify the analysis, all distances were measured in perpendicular cross-sections from an OCT pull-back in the MV, and not taken from the longitudinal images (which is very difficult). The malapposition distance in the half toward the SB of the bifurcation segment was measured as in the straight segments: from an OCT pull-back in the MV, the measurement was taken for the shortest distance between malapposed/floating strut and vessel wall. When using the complex technique, MV and SB stents differed in their strut thickness. The SB stent is the outer stent, the MV stent the inner one, thus malapposed struts are likely to belong to the MV stent at the level of bifurcation and in the proximal segment. Strut malapposition was calculated on the basis of the MV stent type and strut thickness.

Cardiac Biomarkers

Peri-procedural myocardial infarction (MI), with or without pathological Q waves, was defined as a post-procedural Troponin I elevation of ≥3 times the upper limit of normal (0.04 μg/L).

Statistical Analysis

The presence of normal distribution of continuous variables was assessed by means of visual estimation of their frequency histogram and with the use of the Shapiro-Wilk test. Continuous variables are expressed as mean (standard deviation [SD]) or median and interquartile range (IQR) if they followed a normal or non normal distribution, respectively. Categorical variables are expressed as frequency and percentage. In the overall population, differences of continuous variables among the four segments within the lesion were assessed with Kruskal-Wallis test, because of the presence of non normal distribution of continuous variables. Comparisons between two groups were performed using Mann Whitney *U* test, as appropriate. A value of 2 tailed $P<.05$ was considered statistically significant. If a significant difference (ie, $P<.05$) was found across the 4 groups we performed 2×2 multiple comparisons with Bonferroni's correction with the level of statistical significance achieved at *P* value <.05/number of comparisons, thus corresponding to <.05/6, $P<.0083$. Categorical variables were analyzed using the χ^2 test or Fisher's exact test, as appropriate. The effect of the strategy type (complex vs simple), the different segments expressed as categorical variables and the interaction between the strategy type and the 4 segments on strut vessel wall separation distance was assessed using mixed effect linear regression analysis, to account for the correlated nature of the data: ie, the presence of segments within a lesion, and of multiple struts within segments. Briefly, 3 levels were considered: level 1=the single strut,

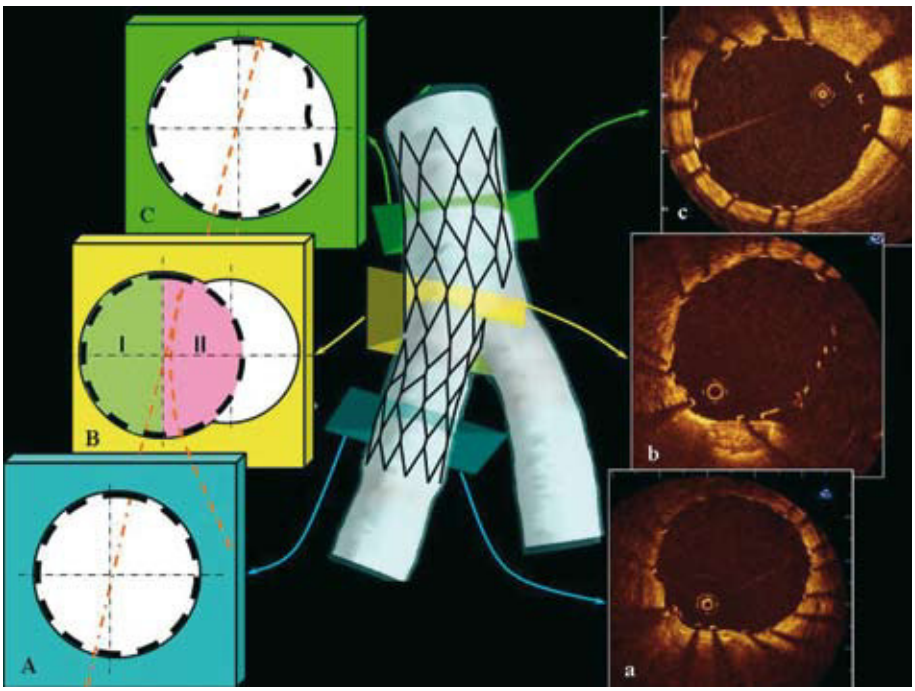

Figure 1. The scheme representing sequential cross-sections of distal segment-A, bifurcation-B and proximal segment-C after bifurcation treatment with simple technique. At the level of bifurcation, cross-section has been divided into 2 halves: I-half opposite side branch, II-half toward side branch. In the proximal main vessel, strut apposition was assessed up to 8 mm before the bifurcation and in the distal main vessel up to 4 mm beyond the bifurcation. On the right side there are corresponding optical coherence tomography cross-sections (a-c).

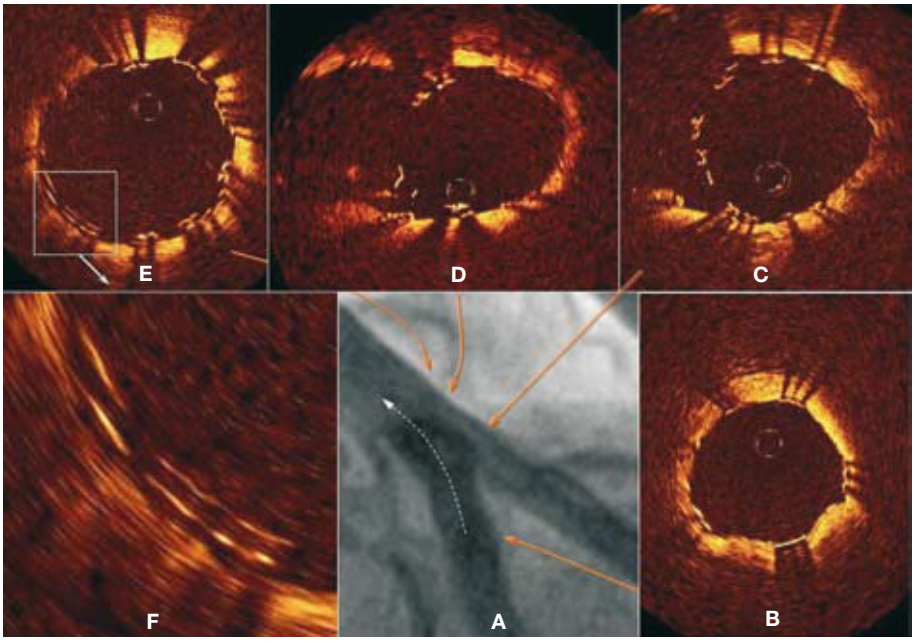

Figure 2. A: angiographic result after implantation of 2 stents into the left anterior descending artery and diagonal branch (Culotte technique). The white arrow indicates the track of the optical coherence tomography imaging wire. Optical coherence tomography images. B: distal segment with well apposed struts. C and D: bifurcation region with malapposed/floating struts in the half facing the side branch. E: well apposed 2 layers of struts in the proximal segment. F: magnification of the 2 layers of struts from image E.

level 2=the segment (proximal, distal, bifurcation half toward SB and half opposite SB), level 3=the lesion, adding the presence/absence of malapposed struts toward SB location as a random effect at level 1. As the percentage of malapposed struts was not expressed at the strut level, Ancova analysis, with weighted least squares as the estimator to correct for heteroskedasticity, was used for this endpoint, after logarithmic transformation, provided adjusted p values. If a significant effect of the type of strategy or of its interaction with the 4 segments was found on the endpoint, 2×2 multiple comparisons between

TABLE 1. **Baseline Patient Clinical Characteristics**

	Simple Technique (n=13)	Complex Technique (n=14)	*P*
Male, n (%)	12 (92)	8 (57)	.08
Age, mean (SD), y	69 (61-73)	70 (62-75)	.59
Diabetes mellitus, n (%)	3 (23)	6 (43)	.42
Hypertension, n (%)	7 (54)	12 (86)	.10
Current/former smoker, n (%)	8 (62)	10 (71)	.69
Family history of CAD, n (%)	8 (62)	11 (85)	.38
Dyslipidemia,a n (%)	12 (92)	12 (86)	1
Previous MI, n (%)	4 (33)	2 (14)	.37
Previous CABG, n (%)	2 (15)	0 (0)	.22
Previous PCI, n (%)	3 (23)	3 (21)	1
Clinical presentation			.21
Stable angina pectoris, n (%)	11 (85)	8 (57)	
ACS, n (%)	2 (15)	6 (43)	

[a]Total cholesterol ≥5 mmol/L or treatment with a lipid lowering drug.
ACS indicates acute coronary syndrome; CABG, coronary artery by-pass graft surgery; CAD, coronary artery disease; MI, myocardial infarction; NSTEMI, non Q-wave myocardial infarction; PCI, percutaneous coronary intervention; SD, standard deviation.

corresponding segments in the simple and complex group were performed. Bonferroni's correction was applied (*P*<.05/10). All analyses were performed using STATA 10.1 statistical software (Statacorp, Texas, USA).

RESULTS

Baseline Clinical Characteristics

Baseline demographics and clinical data are presented in Table 1. Twenty-seven patients (age 69 [61-73] years) with 31 bifurcation lesions were included in the study. Four patients had 2 bifurcations treated. Most of the patients (70%) presented with stable angina at hospital admission.

Angiographic and Procedural Characteristics

Table 2 summarizes angiographic and procedural data according to the treatment strategy: 17 lesions (55%) underwent a simple treatment and 14 (45%) underwent complex bifurcation treatment. Overall, 26 of 31 stents (83.9%) implanted in the MV were DES. Nine of 14 SB stents (64.3%) used in the complex technique were dedicated bifurcation stents: 4 Tryton, 3 bare metal stents (21.4%) and 2 DES (14.3%). The bifurcation target lesion was most frequently located at the left anterior descending/diagonal artery (LAD/Dg), n=17 (55%), followed by the circumflex/obtuse marginal artery (LCx/Om), n=13 (42%), with the right coronary artery/posterior descending (RCA/PDA) in 1 case (3%). The location of the target lesion differed between the two treatment arms, with LAD/Dg lesions being more frequent (86% vs 29%) and LCx/Om lesions less frequent (14% vs 65%) in the complex strategy arm compared to the simple strategy arm. The complex technique was more frequently utilized to treat bifurcation lesions with SB disease: SB diameter stenosis ≥50% (79% vs 12%, *P*<.001), larger SB diameter stenosis (63% vs 29%, *P*=.001), SB minimal lumen diameter (0.8 mm vs 1.4 mm; *P*=.007) and SB lesion length (5.6 mm vs 2.9 mm; *P*=.04). There were no differences in treatment strategy with respect to SB reference lumen diameter.

True bifurcation lesions were present in 13 of 31 bifurcation lesions (42%). Eleven of 13 true bifurcation lesions (85%) were treated with the complex technique and only 2 true bifurcation lesions (15%) were treated with the simple technique (*P*<.001). Significantly higher balloon pressure was applied for SB post-dilatation when a complex technique was used (15 atmospheres vs 11.2 atmospheres; *P*=.04). Procedural success (TIMI 3 flow in both branches and SB residual diameter stenosis <50%) was achieved in all cases. Small procedure-related MI occurred in both groups without significant difference (76.5% v. 100 %; *P*=.1).

Longitudinal Distribution of Malapposed Struts

The OCT analysis is presented in Figures 3 and 4. In total, 8666 struts were evaluated: 4281 (49.4%) in the proximal vessel segment, 1434 (16.5%) at the bifurcation level, and 2951 (34.1%) in the distal vessel segment. The prevalence of malapposed struts was significantly higher at the level of bifurcation in the half toward SB (46.1% [35.3-62.5]) as compared to the bifurcation half opposite SB (9.1% [2.2-21.6];

TABLE 2. **Angiographic and Procedural Data (per Lesion))**

Variable	Simple Technique (n=17)	Complex Technique (n=14)	*P*
Number of diseased vessels			.021
One vessel, n (%)	6 (35)	8 (57)	
Two vessels, n (%)	2 (12)	5 (36)	
Three vessels, n (%)	9 (53)	1 (7)	
Target vessel bifurcation			.007
LAD/Dg, n (%)	5 (29)	12 (86)	
LCx/OM, n (%)	11 (65)	2 (14)	
RCA/PDA, n (%)	1 (6)	0	
Medina classification, n (%)			.009
0,1,0	9 (53)	1 (7)	
1,0,0	4 (23)	1 (7)	
0,1,1	1 (6)	3 (21)	
1,0,1	1 (6)	3 (21)	
1,1,0	2 (12)	1 (8)	
1,1,1	0 (0)	5 (36)	
True bifurcation, n (%)	2 (12)	11 (79)	<.001
Baseline reference vessel diameter, mean (SD), mm			
Proximal MV	3.1 (0.8)	3.0 (0.9)	.7
Distal MV	2.6 (0.8)	2.2 (0.6)	.2
SB	2.0 (0.6)	2.1 (0.5)	.7
Initial diameter stenosis, mean (SD),%			
Proximal MV	45 (29)	54 (24)	.4
Distal MV	55 (28)	56 (35)	.9
SB	29 (21)	63 (30)	.001
Baseline minimal lumen diameter, mean (SD), mm			
Proximal MV	1.7 (0.9)	1.4 (0.7)	.3
Distal MV	1.1 (0.8)	1.0 (0.9)	.7
SB	1.4 (0.6)	0.8 (0.7)	.007
Lesion length, mean (SD), mm			
Proximal MV	4.6 (4.6)	5.8 (5.5)	.5
Distal MV	6.1 (7.6)	8.6 (8.2)	.4
SB	2.9 (1.5)	5.6 (4.7)	.04
Calcified lesions, n (%)	6 (35)	5 (36)	1
Maximal balloon pressure, mean (SD), atm			
MV	13.9 (5.5)	17.1 (5)	.1
SB	11.2 (4.7)	15.0 (3.4)	.04
Type of stent implanted in the MV, n (%)			.4
Paclitaxel eluting stent (Taxus)	6 (35)	5 (36)	
Paclitaxel eluting stent (Costar)	0	1 (7)	
Rapamycin eluting stent (Cypher)	4 (23)	5 (36)	
Zotarolimus eluting stent (Endeavor Resolute)	1 (6)	1 (7)	
Everolimus eluting stent (Xience V)	1 (6)	2 (14)	
BMS (Antares)	4 (24)	0	
BMS (Driver)	1 (6)	0	
Total MV stent length, mean (SD), mm	31.8 (18.5)	33.8 (19.3)	.8
MLD after procedure, mean (SD), mm			
Proximal MV	3.1 (0.6)	3.2 (0.6)	.8
Distal MV	2.7 (0.5)	2.5 (0.5)	.4
SB	1.9 (1)	2.1 (0.4)	.4
Diameter stenosis after procedure, mean (SD), %			
Proximal MV	7 (6)	7 (9)	.8
Distal MV	8 (6)	7 (8)	.8
SB	20 (22)	9 (11)	.1
Final KB, n (%)	15 (88)	14 (100)	.5
IIb/IIIa inhibitor, n (%)	1 (6)	2 (14)	.4
Post-procedural Troponin I rise, µg/L (SD	1.2 (1.6)	2.4 (5.4)	.6
Post-procedural MI, n (%)	13 (76.5)	14 (100)	.1

BMS indicates bare metal stent; Dg, diagonal branch; KB, kissing balloon; LAD, left anterior descending artery; LCx, left circumflex artery; MI, myocardial infarction; MLD,-minimal lumen diameter; MV, main vessel; OM, obtuse marginal branch; PDA, posterior descending artery; RCA, right coronary artery; SB, side branch; SD, standard deviation.

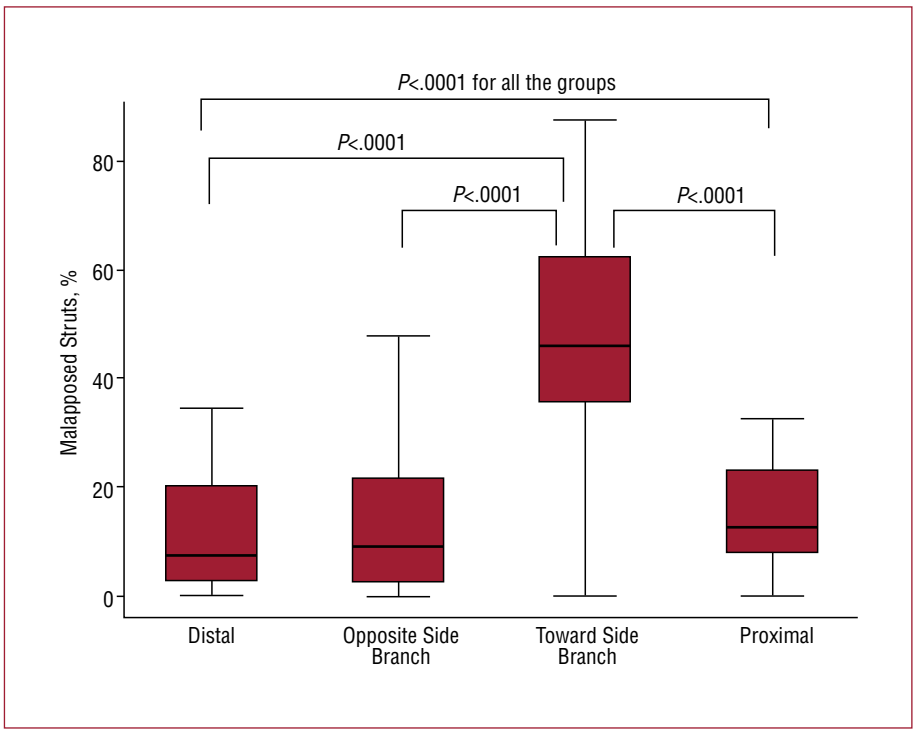

Figure 3. Longitudinal distribution of % of malapposed struts across 4 segments: distal, bifurcation half opposite side branch, bifurcation half toward side branch, proximal. Only significant P values are reported.

P<.0001), the distal segment (7.5% [2.3-20.2]; *P*<.0001, adjusted-*P*), and the proximal segment (12.6 [7.8-23.1]; *P*<.0001), with no significant difference between proximal and distal segments (*P*=.07), bifurcation half opposite SB and proximal segment (*P*=.22), bifurcation half opposite SB and distal segment (*P*=.76) (*P*=.0001 Kruskal Wallis among 4 groups [Figure 3]; Ancova adjusted *P*<.0001). The strut vessel wall distance for malapposed struts was higher toward the SB (98 µm, [37-297]) as compared to the opposite SB (31 µm, [13-74]; *P*<.0001), the proximal segment (49 µm, [20-100]; *P*<.0001) and distal segment (38 µm [17-90]; *P*<.0001]), higher in proximal segment as compared to distal segment (*P*=.0082), and to opposite SB (*P*=.0019), with no significant difference between opposite SB and distal segment (0.23) (*P*=.0001 Kruskal Wallis for the comparison among 4 groups, Figure 4) (20.5 µm, 95% CI, 6.8-34.2; *P*=.003 at mixed effect linear regression analysis).

OCT Analysis: Differences Between Simple and Complex Techniques

Both the overall number of struts per patient and the number of struts in the proximal segment were significantly higher with complex stenting than with a simple technique (323 [97] vs 243 [102]; *P*=.036 and 175 [18] vs 107 [64]; *P*=.015, respectively). The prevalence of malapposed struts and strut vessel wall separation distance, in the 2 groups is shown in Table 3. Regarding the endpoint of the percentage of malapposed struts, Ancova analysis showed that the use of a complex strategy (*P*=.31) and the interaction between complex strategy and the 4 segments (*P*=.75) were not significant. Indeed, no significant difference was found between proximal segments (*P*=.56), distal segments (*P*=.95), segments opposite SB (*P*=.20), and segments toward SB (*P*=.68). Regarding strut vessel wall distance, mixed effect linear regression analysis showed that the interaction between complex strategy and the 4 segments of the lesion was significant (-9.3 µm; 95% CI, -17.9 to 0.7; *P*=.033), while the use of the complex strategy was not significant (3.4 µm; 95% CI, -31.3 to 38.1; *P*=.85), indicating that the complex strategy was associated with a lower strut vessel wall distance at specific segments. Indeed, strut vessel wall separation distance was significantly lower at the proximal segment in the complex group as compared to the simple group (*P*=.0008), without significant difference between distal segments (*P*=.25), segments opposite SB (*P*=.083), and segments toward SB (*P*=.0878).

DISCUSSION

Angiography evaluates only the vessel lumen and therefore has a very limited ability to recognize the adequacy of stent expansion and wall apposition.

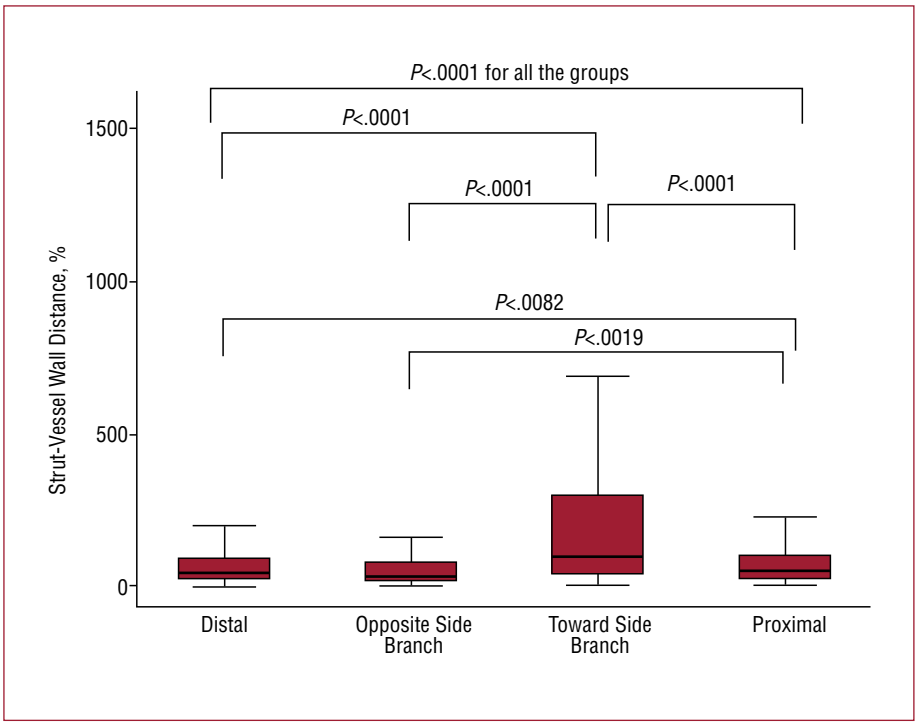

Figure 4. Longitudinal distribution of strut-vessel wall distance across 4 segments: distal, bifurcation half opposite side branch, bifurcation half toward side branch, proximal. Only significant P values are reported.

TABLE 3. **OCT Data According to Simple and Complex Technique**

	Simple Technique (n=17)	Complex Technique (n=14)	*P*
Final OCT MLA, mean (SD), mm²			
Proximal	8.1 (2.6)	9.2 (1.6)	.19
Bifurcation	8.5 (2.4)	9.4 (1.9)	.28
Distal	6.6 (2.3)	6.1 (1.8)	.57
Malapposed struts, %, median (25-75)			
Proximal	11.8 (5.1-23.1)	15.5 (9.4-22.9)	.56
Opposite SB	5.91 (0-17.6)	14.2 (9.1-21.6)	.20
Toward SB	45.4 (35.3-54.5)	50.3(35.3-62.5)	.68
Distal	7.5 (2.3-20.2)	7.9 (2.9-14.3)	.95
Malapposed strut-vessel wall distance, µm, median, (25-75)			
Proximal	60 (20-170)	47 (21-81)	.0008
Opposite SB	21 (8-87)	37 (20-71)	.083
Toward SB	81 (30-267)	123 (41-333)	.088
Distal	38 (17-101)	31 (13-80)	.25

OCT, optical coherence tomography; OCT MLA, optical coherence tomography minimal lumen area; SB, side branch; SD, standard deviation.

IVUS allows good assessment of stent expansion, but for the detection of stent apposition, its low resolution (about 120 µm) is insufficient to quantify this phenomenon precisely. IVUS data from the Sirolimus-Eluting Stent (SES) in the De Novo Coronary Lesions (SIRIUS) trial showed that post-procedural incomplete stent apposition (ISA) was present in 16.2% of 80 SES implantations.[15] A similar incidence of ISA was shown in the IVUS studies by Kimura et al. after implantation of SES in 168 patients (18%)[16] and by Kim et al. after implantation of paclitaxel-eluting stent (PES) and SES in 299 patients (13.9%).[17] However, IVUS may potentially underestimate the prevalence of strut malapposition: in a study comparing IVUS and OCT in 27 patients undergoing PCI, Hou et al. found that IVUS identified stent malapposition in only 10.5% as opposed to 63.2% of cases when

assessed by OCT.[18] Additionally, instead of assessing the prevalence of stent strut malapposition as by OCT, previous IVUS analyses only assessed how many patients had at least one malapposed strut. Finally, previous IVUS analyses have specifically excluded bifurcation segments from the assessment of incomplete stent apposition, rightly assuming that malapposition was unavoidable at that level.[15] Indeed, only a few IVUS analyses have addressed the results of bifurcation stenting and they have focused on poor expansion rather than malapposition. Costa et al. performed post-intervention IVUS assessment in 40 patients treated with the "crush" technique, and found ISA in more than 60% of cases, mainly proximal to the bifurcation where 3 layers of stents were present.[19]

Detailed OCT comparison in the present study showed a much higher incidence of malapposition per lesion. We believe that the prominent artifacts induced by the stent struts with IVUS limit the visualization of the underlying wall, impairing the ability to detect minor degrees of malapposition. The complex 3-dimensional geometry of bifurcation lesions makes it difficult to achieve strut apposition comparable to that observed in a straight segment. In vitro model studies have previously demonstrated the difficulty in achieving good stent apposition at the SB ostium, regardless of which stenting technique is used.[20] Malapposed struts often create a metallic neo-carina both at the proximal and the distal end of often eccentric SB openings (Figure 2). Rewiring the SB in the most distal stent cell close to the carina was consistently attempted, crossing the stent with a looped wire pulled back to the bifurcation. Even when this is achieved, a balloon diameter exactly matching the ostium of the SB inflated at a pressure sufficient to displace all struts is required. In previous OCT observations, the rate of malapposed struts following the treatment of simple lesions in straight vessel segments was 9%,[7] while the rate of malapposed struts in overlapping stents was as high as 41.8%, compared with 20.1% and 9.7% in non-overlapping proximal and distal segments, respectively.[14]

Although pathology studies suggest that stent malapposition is a potential contributor toward adverse events, there are discrepancies when it comes to establishing the prognostic implication of ISA from the only available IVUS studies. Available data are mainly driven from the IVUS sub-studies of the initially highly selected DES studies in straight segments with the exclusion of bifurcation lesions. Similar stent malapposition rates were observed in patients who developed adverse events and in those without adverse events.[21] Others have demonstrated a higher prevalence of abnormal IVUS findings regarding stent apposition and expansion following stent implantation in patients who developed acute stent thrombosis as compared to a control group.[19]

Surprisingly, our study did not show any significant differences between the simple and complex techniques with regard to strut malapposition; with a complex technique one could theoretically expect higher rates of malapposed struts simply because of more metal inserted. These findings may be explained by more aggressive KB post-dilatation in two-stents techniques than in a one-stent strategy, without fear of causing dissection and thereby compromising the SB. Also the predominant usage of a dedicated bifurcation stent in our series may have played a role, although a comparison between different types of stents within the Culotte group cannot be performed given the small sample size.

Pathology studies have shown that arterial branch points are foci of low shear and low flow velocity and are sites predisposed to the development of atherosclerotic plaque and thrombus.[22] The important observation was that the most vulnerable bifurcation area is located opposite the flow divider.[23] Since SB dilatation through the stent struts may cause deformation of the MV stent,[6] it is prudent to focus careful attention not only on the carina (one could expect the worst strut apposition at this site, a finding which we have corroborated), but also on strut apposition opposite the flow divider, where lower shear stress might possibly serve as a nidus for restenosis or thrombosis.[24] Our observations did not show an increased rate of malapposed struts in the half opposite SB as compared to non-bifurcation segments (proximal and distal to the bifurcation), although this may be explained by the high rate of KB post-dilatation.

Healing of Malapposed Struts

The prognostic implication of suboptimal acute strut apposition following PCI as assessed by OCT, in patients with satisfactory angiographic images, is unknown.

Final Kissing Balloon Post-Dilatation

Since the simple technique may cause SB narrowing via carina displacement[25] while dilatation of the SB leads to distortion of the MV stent,[6] final KB is highly recommended when treating bifurcation lesions. The beneficial role of final KB is supported by previous clinical observations.[26] However, bench-tests indicate that final KB inflation may decrease, but not necessarily eliminate, strut-vessel wall separation.[27]

Limitations

The main limitation is the lack of statistical analysis that could fully account for the correlated OCT data, that presents a hierarchical structure with more lesions clustered in the same patients, 4 segments within a single lesion, more struts within the same segment, for each endpoint analyzed. Formal sample size calculations are difficult in this situation and no power calculation algorithm exists that is based on generally accepted assumptions regarding intra-cluster correlation design factors. The lack of randomization to a simple or complex technique might have created bias in the study results. Indeed, a complex technique tended to be selected for true bifurcations while a simple technique was reserved for other bifurcation lesion subtypes. Secondly, we used different stent types (including dedicated bifurcation stents for treatment of a part of the SB lesions in the complex technique), each with a unique geometry and cell size, which might also have influenced our findings. Therefore we cannot rule out the existence of a small difference in the prevalence of malapposed struts and stent vessel wall separation distance between the two techniques, due to the lack of statistical power. Thirdly, the findings cannot necessarily be applied to other two-stents techniques for the bifurcation treatment, except those from the Culotte stenting. Finally, OCT imaging was acquired only from the MV. This obviously penalizes the simple technique results because malapposed struts in the SB are not detected. In this study OCT was used only at the end of the angiographically guided optimization of stent deployment.

CONCLUSIONS

In coronary bifurcation lesions, strut malapposition occurs most frequently and is most severe at the level of the SB origin. Our findings suggest that the use of complex technique (Culotte) does not significantly affect the rate of strut malapposition across the four segments of bifurcation lesions and is associated with a lower strut vessel wall separation distance of malapposed struts at the proximal segment as compared to a simple strategy of stenting the main vessel only. Whether malapposition may play a role in the high incidence of in-stent restenosis or stent thrombosis affecting bifurcation lesions, needs to be assessed in further studies.

REFERENCES

1. Capodanno D, Capranzano P, Bucalo R, Sanfilippo A, Ruperto C, Caggegi A, et al. A novel approach to define risk of stent thrombosis after percutaneous coronary intervention with drug-eluting stents: the DERIVATION score. Clin Res Cardiol. 2009;98:240-8.
2. Iakovou I, Schmidt T, Bonizzoni E, Ge L, Sangiorgi GM, Stankovic G, et al. Incidence, predictors, and outcome of thrombosis after successful implantation of drug-eluting stents. JAMA. 2005;293:2126-30.
3. Hoye A, Iakovou I, Ge L, van Mieghem CA, Ong AT, Cosgrave J, et al. Long-term outcomes after stenting of bifurcation lesions with the "crush" technique: predictors of an adverse outcome. J Am Coll Cardiol. 2006;47:1949-58.
4. Hildick-Smith D, de Belder AJ, Cooter N, Curzen NP, Clayton TC, Oldroyd KG, et al. Randomized trial of simple versus complex drug-eluting stenting for bifurcation lesions: the British Bifurcation Coronary Study: old, new, and evolving strategies. Circulation. 2010;121:1235-43.
5. Jensen JS, Galløe A, Lassen JF, Erglis A, Kumsars I, Steigen TK, et al. Nordic-Baltic PCI Study Group. Safety in simple versus complex stenting of coronary artery bifurcation lesions. The nordic bifurcation study 14-month follow-up results. EuroInterv. 2008;4:229-33.
6. Ormiston JA, Webster MWI, El Jack S, Ruygrok PN, Stewart JT, Scott D, et al. Drug-Eluting Stents for Coronary Bifurcations: Bench Testing of Provisional Side-Branch Strategies. Catheter Cardiovasc Interv. 2006;67:49-55.
7. Tanigawa J, Barlis P, Dimopoulos K, Dalby M, Moore P, Di Mario C. The influence of strut thickness and cell design on immediate apposition of drug-eluting stents assessed by optical coherence tomography. Int J Cardiol. 2009;134:180-8.
8. Tyczynski P, Ferrante G, Kukreja N, Moreno-Ambroj C, Barlis P, Ramasami N, et al. Optical Coherence Tomography assessment of a new dedicated bifurcation stent. Eurointerv. 2009;5:544-51.
9. Chevalier B, Glatt B, Royer T, Guyon P. Placement of coronary stents in bifurcation lesions by the "culotte" technique. Am J Cardiol. 1998;82:943-9.
10. Colombo A, Bramucci E, Saccà S, Violini R, Lettieri C, Zanini R, et al. Randomized study of the crush technique versus provisional side-branch stenting in true coronary bifurcations: the CACTUS (Coronary Bifurcations: Application of the Crushing Technique Using Sirolimus-Eluting Stents) Study. Circulation. 2009;119:71-8.
11. Medina A, Suarez de Lezo J, Pan M. A new classification of coronary bifurcation lesions. Rev Esp Cardiol. 2006;59:183.
12. Goktekin O, Kaplan S, Dimopoulos K, Barlis P, Tanigawa J, Vatankulu MA, et al. A new quantitative analysis system for the evaluation of coronary bifurcation lesions: comparison with current conventional methods. Catheter Cardiovasc Interv. 2007;69:172-80.
13. Kataiwa H, Tanaka A, Kitabata H, Imanishi T, Akasaka T. Safety and usefulness of non-occlusion image acquisition technique for optical coherence tomography. Circ J. 2008; 72:1536-7.
14. Tanigawa J, Barlis P, Dimopoulos K, Di Mario C. Optical coherence tomography to assess malapposition in overlapping drug-eluting stents. EuroInterv. 2008;3:580-3.
15. Ako J, Morino Y, Honda Y, Hassan A, Sonoda S, Yock PG, et al. Late incomplete stent apposition after sirolimus-eluting stent implantation: a serial intravascular ultrasound analysis. J Am Coll Cardiol. 2005;46:1002-5.
16. Kimura M, Mintz GS, Carlier S, Takebayashi H, Fujii K, Sano K, et al. Outcome after acute incomplete sirolimus-eluting stent apposition as assessed by serial intravascular ultrasound. Am J Cardiol. 2006;15;98:436-42.
17. Kim YS, Koo BK, Seo JB, Park KW, Suh JW, Lee HY, et al. The incidence and predictors of postprocedural incomplete stent apposition after angiographically successful drug-eluting stent implantation. Catheter Cardiovasc Interv. 2009;74:58-63.
18. Hou JB, Meng LB, Jing SH, Han ZG, Yu H, Yu B. Combined use of optical coherence tomography and intravascular ultrasound during percutaneous coronary intervention in patients with coronary artery disease. Zhonghua Xin Xue Guan Bing Za Zhi. 2008;36:980-4.

19. Costa RA, Mintz GS, Carlier SG, Lansky AJ, Moussa I, Fujii K, et al. Bifurcation coronary lesions treated with the "crush" technique: an intravascular ultrasound analysis. J Am Coll Cardiol. 2005;46:599-605.
20. Murasato Y, Horiuchi M, Otsuji Y. Three-dimensional modeling of double-stent techniques at the left main coronary artery bifurcation using micro-focus X-ray computed tomography. Catheter Cardiovasc Interv. 2007;70:211-20.
21. Fujii K, Carlier SG, Mintz GS, Yang YM, Moussa I, Weisz G, et al. Stent underexpansion and residual reference segment stenosis are related to stent thrombosis after sirolimus-eluting stent implantation: an intravascular ultrasound study. J Am Coll Cardiol. 2005;45:995-8.
22. Glagov S, Zarins C, Giddens DP, Ku DN. Hemodynamics and atherosclerosis. Insights and perspectives gained from studies of human arteries. Arch Pathol Lab Med. 1988;112:1018-31.
23. Gonzalo N, Garcia-Garcia HM, Regar E, Barlis P, Wentzel J, Onuma Y, et al. In vivo assessment of high-risk coronary plaques at bifurcations with combined intravascular ultrasound and optical coherence tomography. JACC Cardiovasc Imaging. 2009;2:473-82.
24. Benard N, Coisne D, Donal E, Perrault R. Experimental study of laminar blood flow through an artery treated by a stent implantation: characterisation of intra-stent wall shear stress. J Biomech. 2003;36:991-8.
25. Vassilev D, Gil RJ. Relative dependence of diameters of branches in coronary bifurcations after stent implantation in main vessel-importance of carina position. Kardiol Pol. 2008;66:371-8.
26. Adriaenssens T, Byrne RA, Dibra A, Iijima R, Mehilli J, Bruskina O, et al. Culotte stenting technique in coronary bifurcation disease: angiographic follow-up using dedicated quantitative coronary angiographic analysis and 12-month clinical outcomes. Eur Heart J. 2008:29;2868-76.
27. Vassilev D, Gil R. Changes in coronary bifurcations after stent placement in the main vessel and balloon opening of stent cells: theory and practical verification on a bench-test model. J Geriatr Cardiol. 2008;5:43-9.